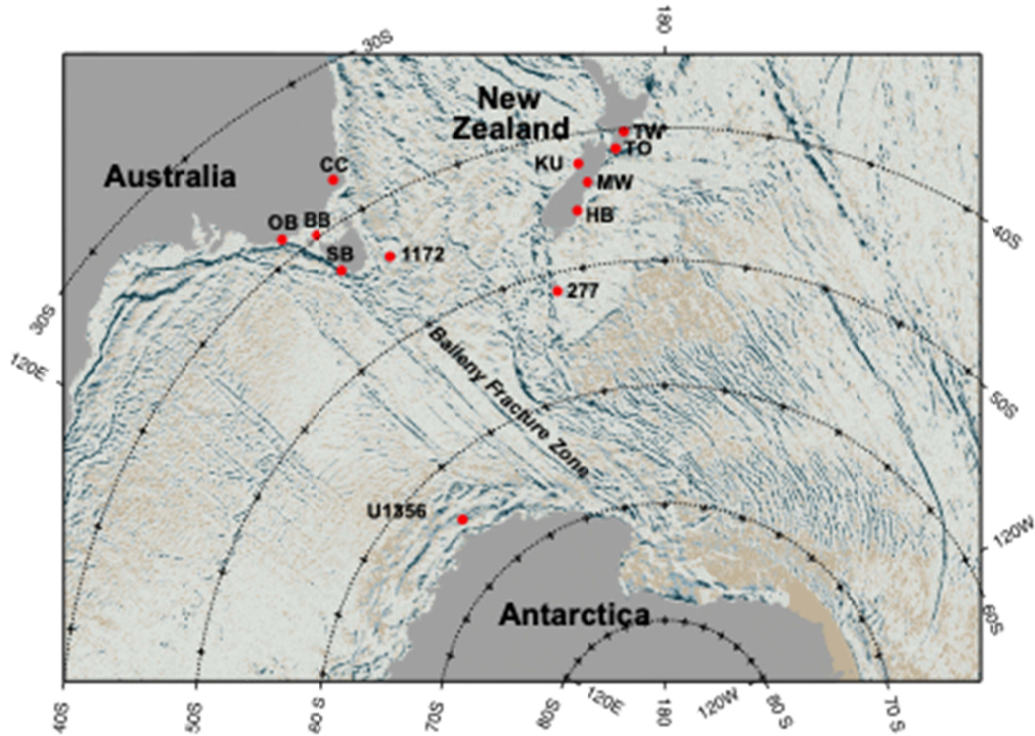1 **Supplementary Text**
2 **Dinocyst assemblages**
3 *Point Margaret*
4 Overall, latest Paleocene dinocyst assemblages (Fig. S8) at Point Margaret are
5 entirely dominated by small Peridinioid taxa, including *Spinidinium*, *Vozzhennikovia*,
6 *Phthanoperidinium* and *Senegalinium*. This suggests a strong fresh-water influence, in
7 line with the general lithological evolution of the site that suggests a trend from high-
8 energy sand dominated facies to silt and mud-dominated pro-delta deposits (Frieling
9 et al., 2018). Across the condensed interval at ~46m open marine taxa (*Spiniferites*,
10 *Cordosphaeridium*, *Glaphyrocysta* and *Apectodinium*) are temporarily abundant,
11 signaling continuous marine influence. At the onset of the CIE, the abundance of
12 *Apectodinium* spikes again, reaching maximum abundance of *ca.* 60% of the
13 assemblage. *Florentinia* consistently occurs within the topmost part of the section, at
14 the body of the CIE. The general assemblage characteristics and evolution, with e.g.
15 the abundant low-salinity tolerant small Peridinioid taxa and a distinct pre-PETM
16 *Apectodinium* abundance are strongly reminiscent of the assemblages at ODP 1172
17 (Sluijs et al., 2011) and several events can be correlated (Figure 3).
18
19 *Latrobe-1*
20 Much of the trends observed at Point Margaret are observed in the Latrobe-1 material
21 as well (Fig. S9), but the dominance of the small Peridinioids is less pronounced and
22 dinocyst concentrations are generally much lower (Frieling et al., 2018). The reduced
23 abundance was previously hypothesized to result from long-term storage (Frieling et
24 al., 2018). Similarly, Peridinioids may be disproportionately affected by this
25 degradation, compared to Gonyaulacoid cysts (e.g. Zonneveld et al., 2019, 2008). We
26 argue this also plays a role in shaping the dinocyst assemblages at Latrobe-1. During
27 the PETM, *Apectodinium* is extremely abundant, with ca. 90% of the assemblage, but
28 *Florentinia* is represented by only a single specimen. Based on the CIE profile, the
29 highest abundance of *Apectodinium* is likely positioned above the top of the Point
30 Margaret outcrop and is therefore missing.
31

33 **Supplementary Figures**

34

35
41 **Figure S1. Modern distribution of localities used in this study.** Abbrevations &
42 numbers as follows: Cambalong Creek (CC), Otway Basin (OB), Bass Basin
43 (BB), Sorrell Basin (SB), Kumara core (KU), Hampden Beach (HB), Mid-
44 Waipara river (MW), Tora (TO), Tawanui (TW) and numbered Deep Sea
45 Drilling Project (DSPD) Site 277, Ocean Drilling Program (ODP) Site 1172 and
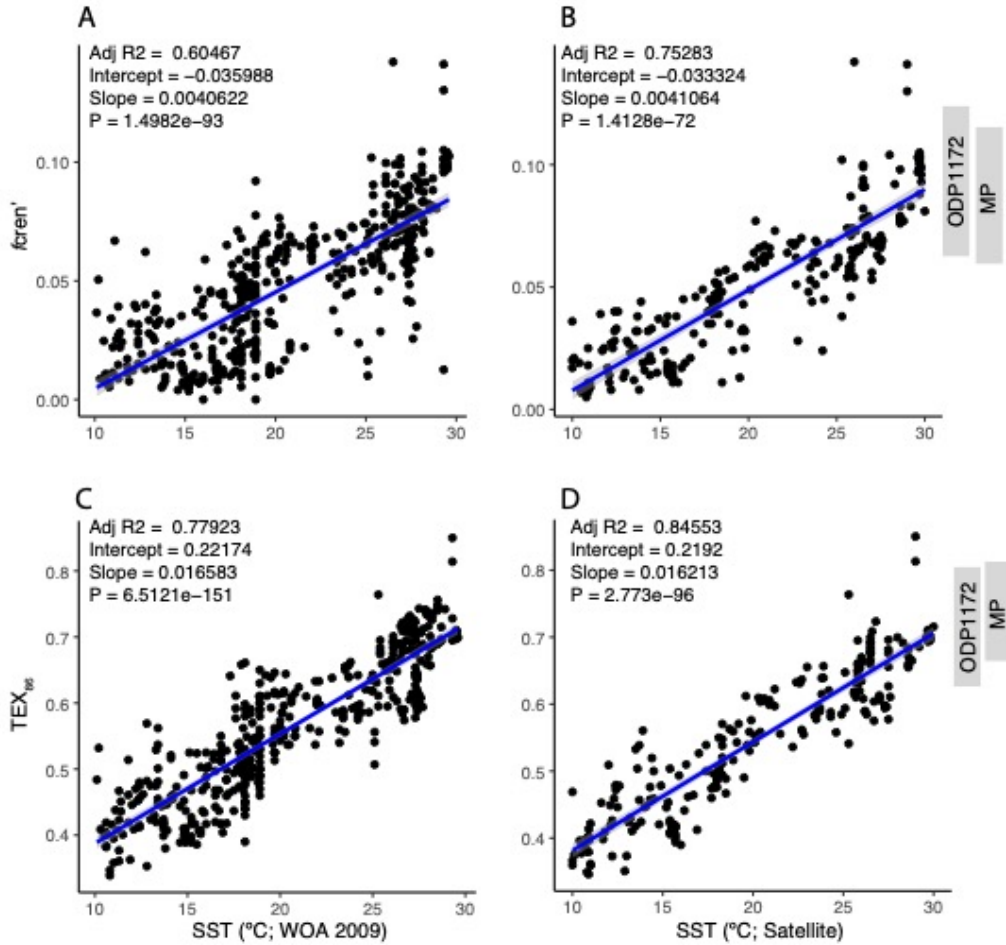46 Integrated Ocean Drilling Program (IODP) Site U1356.

41

Figure S2. Linear correlations of cren'/total crenarchaeol (f(cren')) and TEX$_{86}$ with SST (>10ºC and no Red Sea) in two widely used calibration datasets; Kim et al. 2010 (K2010)(Kim et al., 2010) **and the more expanded Tierney & Tingley 2015 (TT2015)** (Tierney and Tingley, 2015)**.** A. f(cren') in TT2015. B. (fcren') in K2010. C. TEX$_{86}$ vs SST in TT2015. D. TEX$_{86}$ vs SST in K2010. Bars on the right represent the range of observed values for the Paleocene and PETM in the Point Margaret outcrop and Latrobe-1 (MP) and Site 1172 cores. Note that there are only 5 reliable TEX$_{86}$ datapoints in the Point Margaret and 2 in Latrobe-1.
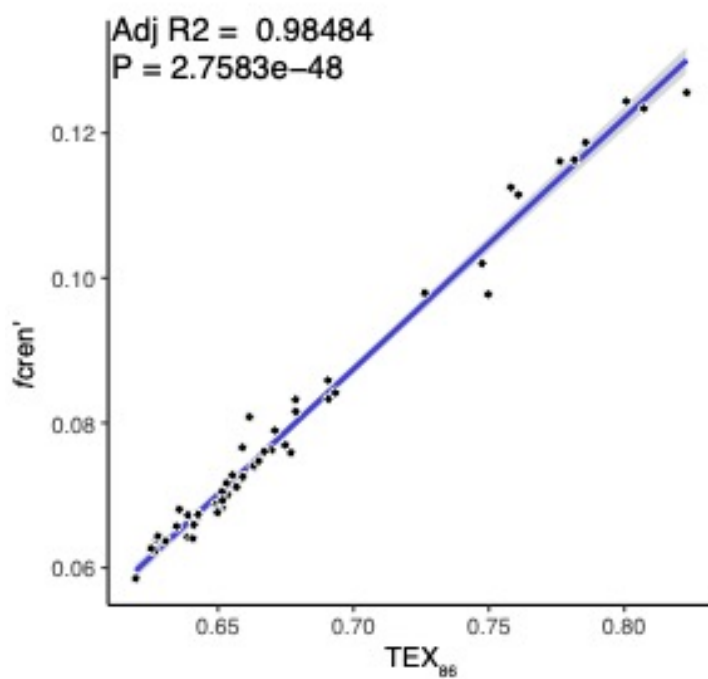
Adj R2 = 0.98484
P = 2.7583e−48

51
52 **Figure S3. Linear correlation between TEX$_{86}$ and $f$cren' at ODP Site 1172 across**
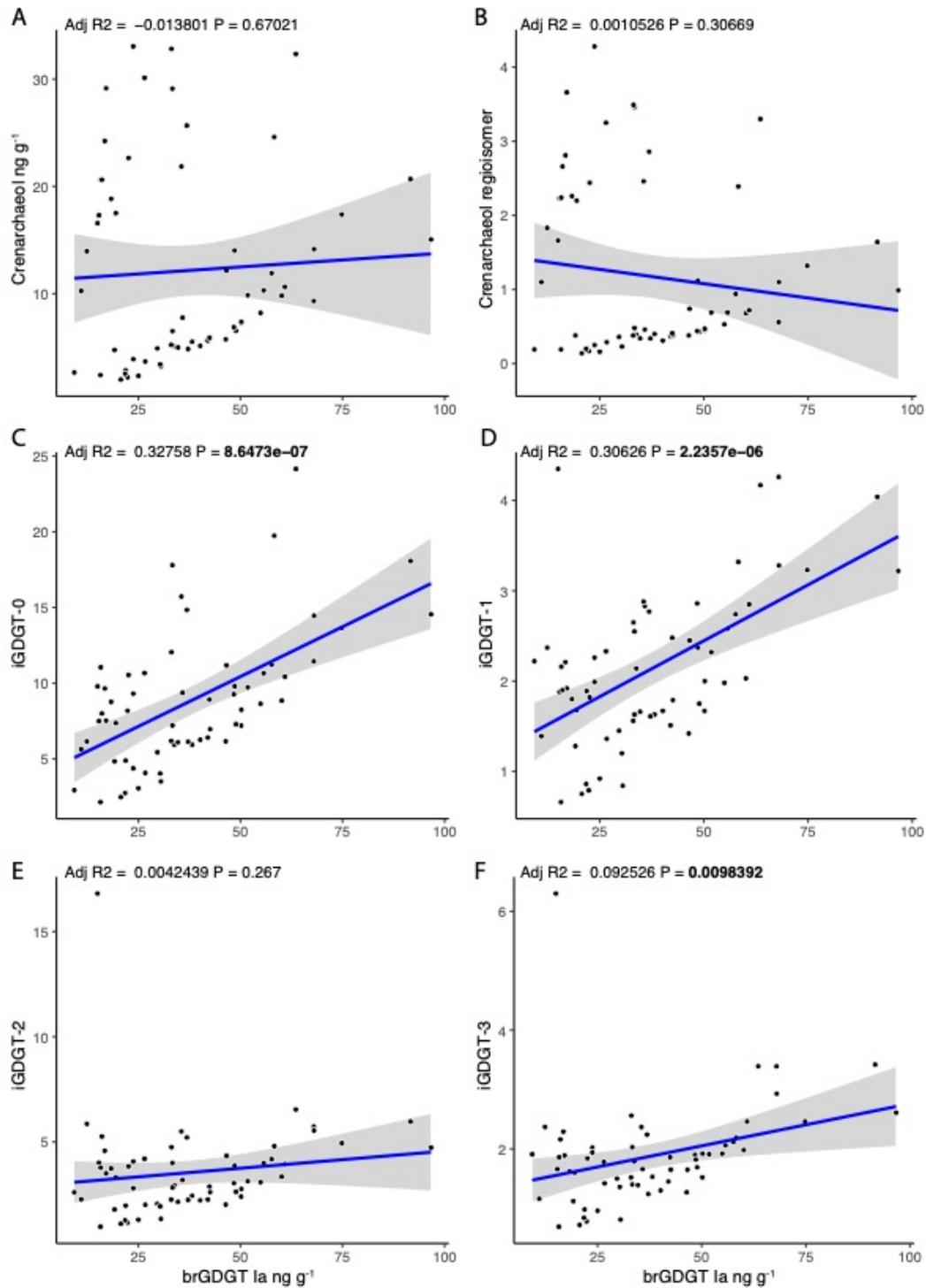53   **the PETM.**
54
55
56

57
58 **Figure S4. Absolute abundances of individual isoprenoid GDGTs compared to**
59 **abundance of the predominant branched GDGT-Ia in ng g^{-1} dry sediment.**
60 A. Crenarchaeol, B. Crenarchaeol isomer, C. GDGT-0, D. GDGT-1, E. GDGT-
61 2, F. GDGT-3. Note that GDGT-0, 1 and 3 show a significant correlation (P <
62 0.01). Units on all axes are measured concentrations.
63

%brGMGT of total brGDGTs
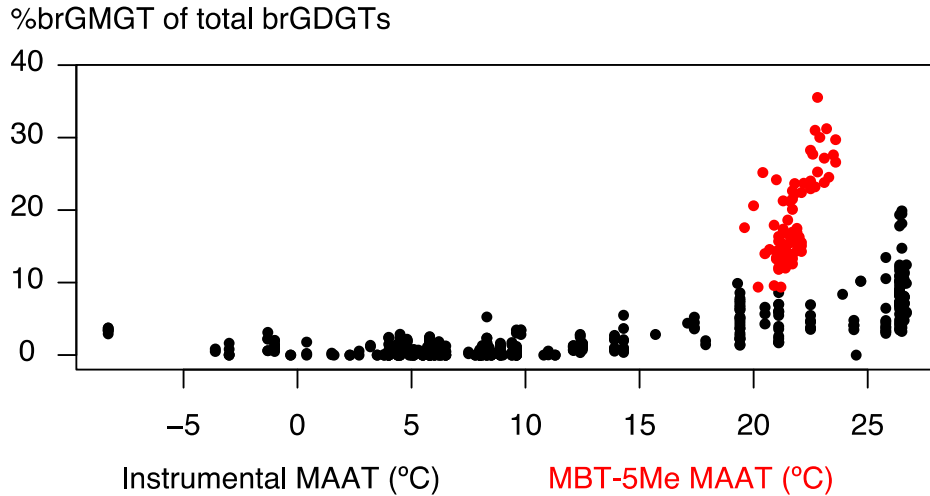

Instrumental MAAT (ºC)　　　MBT-5Me MAAT (ºC)

Figure S5. Abundance of brGMGTs as percentage of total brGMGTs + brGDGTs (%brGMGT). Black dots represent the modern peat database (Naafs et al., 2018), red dots represent the late Paleocene – PETM at Point Margaret (this study). Both datasets are compared to MAAT, which was measured and reconstructed using MBT'$_{5Me}$ for the modern and ancient data, respectively.
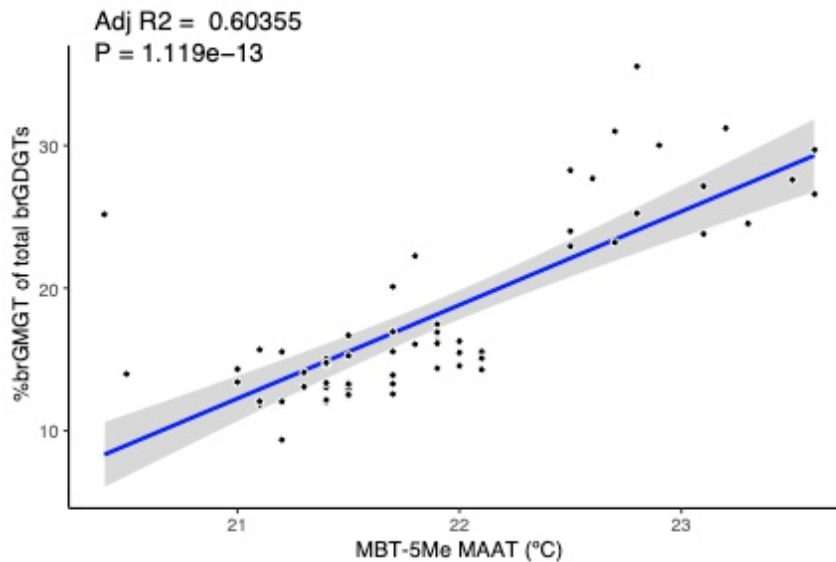

Figure S6. Correlation between %brGMGTs and MBT'$_{5Me}$ derived MAAT at Point Margaret.
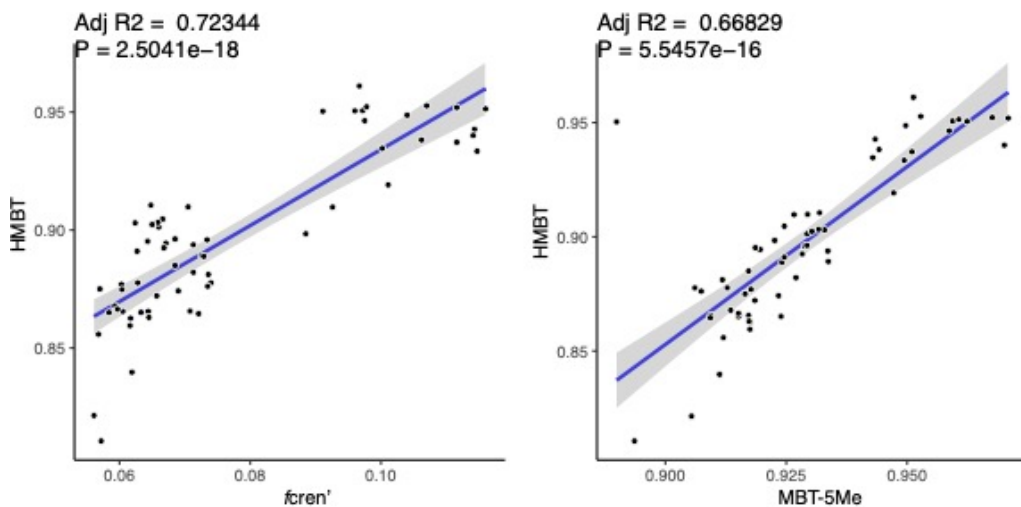
74
75 **Figure S7. Correlation of HMBTacyclic to other lipid biomarker proxies; fcren'**
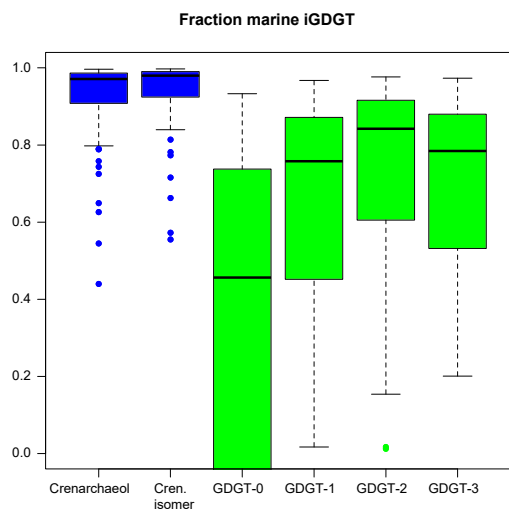76 **and MBT'$_{5Me}$**

77
78 **Figure S8. Average amount of marine contribution to the iGDGT-pool calculated**
79 **following methods described in** Sluijs et al., (2020)**.** The terrestrial fraction in
80 isoGDGT-0 is potentially dominant over the marine in the majority of samples,
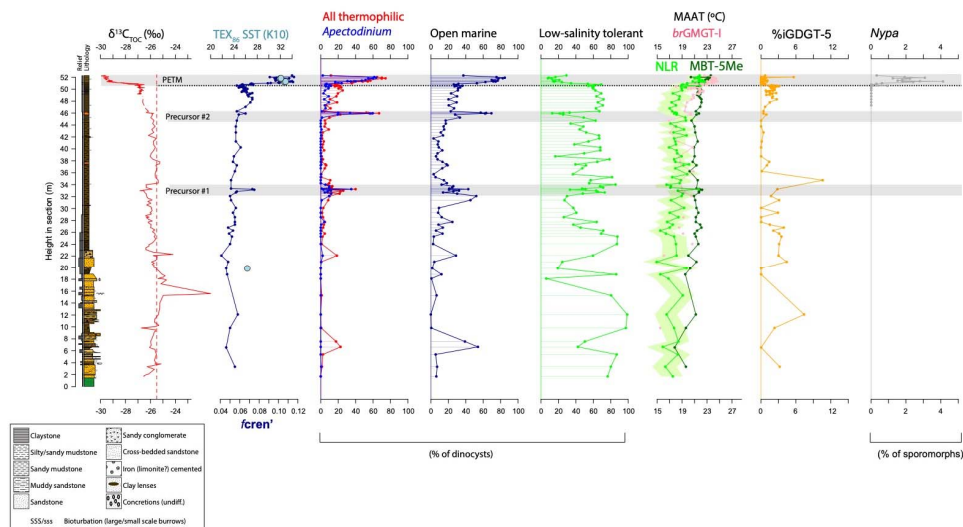81 whereas crenarchaeol and the stereoisomer remain almost exclusively marine.
82

83
84 **Figure S9. Ecological signals based on dinocyst assemblages, pollen and lipid**
85 **biomarker proxy data for the entire Late Paleocene and PETM succession at**
86 **Point Margaret.** Interpretation follows ecological preferences of Frieling & Sluijs
87 (2018; and references therein). See SI data for grouping.
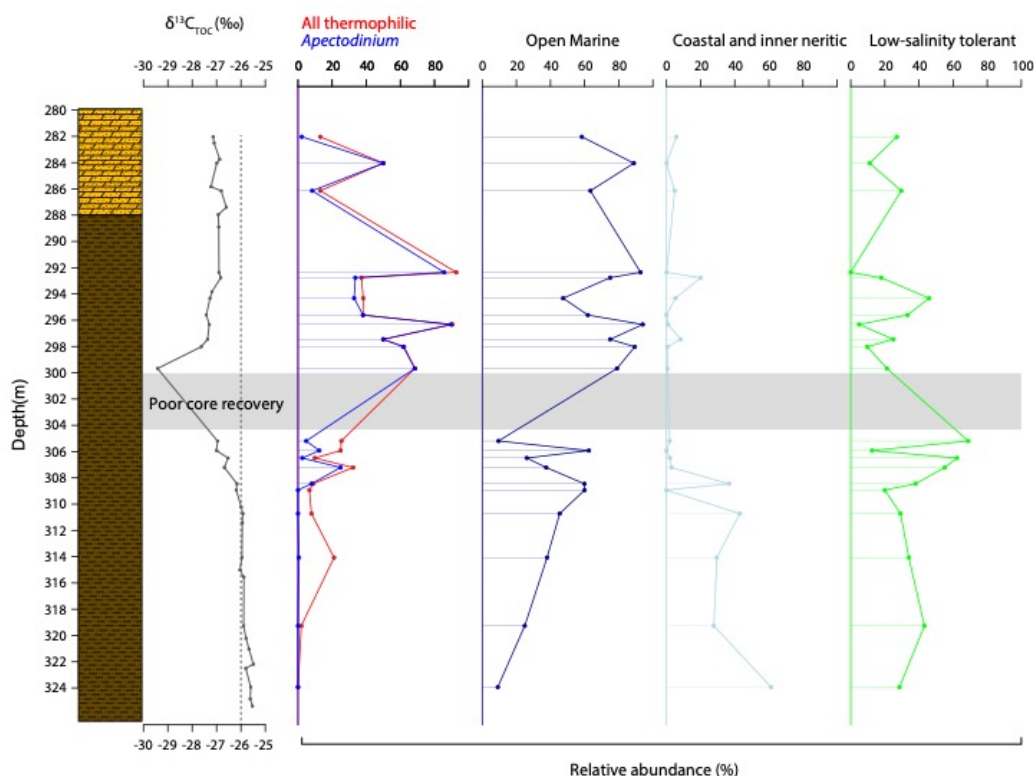88

89
90 **Figure S10. Ecological signals based on dinocyst assemblages for Latrobe-1**
91 **across the PETM.** Interpretation follows ecological preferences of Frieling & Sluijs
92 (2018; and references therein). See SI data for grouping.
93
94